

# The near-field method: a modified equivalent linear method for dynamic soil–structure interaction analysis. Part I: Theory and methodology

Farhad Behnamfar<sup>1</sup> · Hadi Sayyadpour<sup>1</sup>

Received: 21 August 2015 / Accepted: 12 May 2016 / Published online: 28 May 2016  
© Springer Science+Business Media Dordrecht 2016

**Abstract** This paper presents a new direct modeling approach to analyze 3D dynamic SSI systems including building structures resting on shallow spread foundations. The direct method consists of modeling the superstructure and the underlying soil domain. Using a reduced shear modulus and an increased damping ratio resulted from an equivalent linear free-field analysis is a traditional approach for simulating behavior of the soil medium. However, this method is not accurate enough in the vicinity of foundation, or the near-field domain, where the soil experiences large strains and the behavior is highly nonlinear. This research proposes new modulus degradation and damping augmentation curves for using in the near-field zone in order to obtain more accurate results with the equivalent linear method. The mentioned values are presented as functions of dimensionless parameters controlling nonlinear behavior in the near-field zone. This paper summarizes the semi-analytical methodology of the proposed modified equivalent linear procedure. The numerical implementation and examples are given in a companion paper.

**Keywords** Soil–structure interaction · Equivalent linear · Near-field · Shear modulus · Damping

## 1 Introduction

Considering the effects of underlying soil on the response of superstructure is the main purpose of geotechnical earthquake engineering (Bozorgnia and Bertero 2004). The available methods to model the foundation and underlying soil can be classified in two main categories: substructure and direct methods.

---

✉ Farhad Behnamfar  
farhad@cc.iut.ac.ir

Hadi Sayyadpour  
hadisayadpour@gmail.com

<sup>1</sup> Department of Civil Engineering, Isfahan University of Technology, Isfahan 8415683111, Iran

In the substructure method, the soil domain is completely replaced by appropriate elements in order to considering the effects of stiffness and damping of soil on the superstructure. Pais and Kausel (1988), Gazetas (1991), and Mylonakis et al. (2006) presented classical equations for stiffness and damping coefficients of surface and embedded rigid footings. Matlock (1970), Penzien (1970), Nogami et al. (1992), Boulanger et al. (1999), Yim and Chopra (1985), Allotey and El Naggar (2008), and Raychowdhury (2008) used different types of Beam on Nonlinear Winkler Foundation (BNWF) models for analyzing foundations and structures under static and dynamic loading conditions. Plasticity Based Macro-element (PBM) models are recently developed by a number of researchers to capture the nonlinear response of rigid foundations. Some recent versions of PBM models were developed by Cremer et al. (2001), Houlsby and Cassidy (2002), Gajan and Kutter (2008), Chatzigogos et al. (2009, 2011), and Figini et al. (2012).

Unlike the substructure method, the direct method includes modeling the soil domain and superstructure simultaneously and is an application of the finite element method (Gutierrez and Chopra 1978). Modeling the unbounded soil domain, its nonlinear behavior and an enormous computational effort are the most important challenges facing the direct finite element method. Nonlinear behavior of the soil domain can be simulated by different elastic or elastic–plastic constitutive models. Although elastic–plastic constitutive models are more accurate, they usually have many parameters and increase the computational cost. For example, Elgamal et al. (2008) studied three-dimensional (3D) seismic response of the Humboldt Bay Middle Channel Bridge. A nonlinear hysteretic material with a Von Mises multisurface kinematic plasticity model was used to model the foundation soil. They used a special sparse solver and reported 40 h of run time for analyzing the bridge model under a 25 s earthquake excitation. Nonlinear soil structure interaction can involve geometric and material nonlinearities such as structure nonlinearity, uplift, liquefaction etc. Addressing all these issues in the direct method considerably increases the analysis cost. Therefore, efforts have been made to simplify the direct method and make it more practical.

Researchers have shown that just a limited region in the vicinity of structure undergoes considerable plastic deformations; therefore it is not reasonable to use complicated constitutive models to simulate the behavior of the whole soil domain (Wolf and Song 1996). Accordingly, one can divide the soil domain into two parts: a part near the foundation experiencing large strains and nonlinear behavior (the near-field zone) and a remaining part with linear behavior (the far-field zone).

Different methods are available to analyze the near-field and far-field zones. The Boundary Element Method (BEM) can include wave radiation to infinity; therefore, it can be used to model the far-field zone (Von Estorff and Kausel 1989). It seems that using a coupled BEM–FEM method can eliminate the shortcomings of each individual method. Various researchers such as Von Estorff and Kausel (1989), Von Estorff and Firuziaan (2000), Yazdchi et al. (1999), Spyrakos and Xu (2004), Romero et al. (2013), Andersen and Jones (2006), and Vasilev et al. (2015) have presented coupled BEM–FEM methods for dynamic soil–structure interaction problems.

Wolf (2003) developed the Scaled Boundary Finite Element Method (SBFEM) for analyzing bounded and unbounded domains. He suggested that the unbounded far-field to be analyzed with SBFEM while the bounded near-field could be modeled with FEM having nonlinear material properties. Other researchers like Genes and Kocak (2005), Bazyar and Song (2006) and Chen et al. (2015) modified this method for layered and non-homogeneous unbounded domains.

Using the Equivalent Linear Method (ELM) is an effective approach to simplify the direct method and to enhance its efficiency and applicability. In this approach, the soil

domain is assumed to behave linearly both in the near- and far-field zones and its dynamic properties are computed through an equivalent linear analysis (i.e. free-field analysis). An iterative procedure is used in the free-field analysis and the shear modulus and damping of each soil layer are readjusted in every iteration based on the effective shear strain in each different layer (Kramer 1996). When this procedure converges, strain-compatible shear modulus and damping values used for simulating the soil domain are calculated. These values are constant throughout the duration of the earthquake. Cubrinovski and Ishihara (2004), Casciati and Borja (2004) and Manna and Baidya (2010) employed ELM to approximate the nonlinear soil behavior in analyzing different types of structures. Since this method is only applicable for strain levels under approximately one percent (Ishihara 1996), using the equivalent linear properties in the near-field region, will not result in accurate results and it is the serious limitation of the ELM. On the other hand, in the conventional ELM the modified soil properties are obtained through a free-field analysis and therefore, the effects of large strains around the foundation are excluded. In a recently published paper, Ghandil and Behnamfar (2015) resolved this limitation and proposed the near-field method as a modified equivalent linear method with a further reduction of the soil shear modulus in the near-field of foundation resulting in validity of using the equivalent linear method throughout. They considered several 3D buildings resting on different soil types and proposed semi-analytical relations for calculating the shear modulus modification factors as functions of the fixed-base period of structures. Results showed that the near-field method, being more accurate than traditional ELM, can considerably reduce the computational cost of the direct method.

The present study is the continuation of the previous study by Ghandil and Behnamfar (2015). The main objective of this research is to propose an approach to include the nonlinear soil behavior in linear FE models and calculate maximum seismic displacements of building structures resting on shallow spread foundations. Here, the near-field method is generalized to be applicable for a wide range of building structures. To attain this goal, a set of dimensionless parameters representing relative properties of building structures and soil is selected and a comprehensive parametric study is carried out to determine the near-field zone dimensions and capture the variation of near-field properties, including the shear modulus and the damping ratio, with respect to these parameters.

## 2 Key dimensionless parameters

Soil–structure interaction and the effect of various parameters on this phenomenon have been the subject of many researches. Veletsos and Meek (1974), Veletsos and Nair (1975), Bielak (1975) and Wolf (1985) introduced dimensionless parameters that control response of a dynamic soil–structure system under a specific excitation. Table 1 lists these dimensionless parameters. In this table,  $h$  refers to structure height,  $V_S$  is the shear wave velocity of the soil,  $T$  is the fixed-base period of the structure,  $a$  is a characteristic length of the foundation (i.e. half-width or radius of the foundation),  $\omega_S$  refers to structure's angular frequency,  $m$  is the effective modal mass of structure and  $\rho_S$  is the mass density of the soil.

Some researchers like Veletsos and Meek (1974) and Avilés and Pérez-Rocha (1996) studied the influence of the above mentioned parameters and concluded that the inertial SSI effects are more sensitive to the stiffness ratio ( $\bar{s}$ ) and the slenderness ratio ( $\bar{h}$ ) and sensitivity to the mass ratio ( $\bar{m}$ ) is modest. In addition, it was concluded that neglecting other parameters such as linear and rotary inertia of the foundation may be permissible for

**Table 1** Dimensionless parameters that alter the soil–structure interaction effects

Parameter	Description
$\bar{s} = \omega_S h / V_S$ (or $h / V_S T$ )	$\omega_S h$ and $V_S$ quantify the stiffness of the structure and soil, respectively, and then this parameter represents the structure to soil stiffness ratio
$\bar{h} = h / a$	The slenderness ratio (structure's height to foundation width ratio) describing the geometry of the soil–structure system
$\bar{m} = m / \rho_S a^2 h$	$\rho_S a^2 h$ is the mass of soil in a volume extending to a depth equal to the structure height, $h$ , below the foundation. This parameter represents the structure to soil mass ratio
$\xi$	Damping ratio of structure
$\xi_g$	Damping ratio of soil
$\nu$	The Poisson's ratio of soil

deriving effective system parameters (Avilés and Pérez-Rocha 1996). Accordingly,  $\bar{s}$ ,  $\bar{h}$  and  $\bar{m}$  are considered as key dimensionless parameters in this research and the effects of these parameters on the properties of the near-field region are studied.

## 2.1 Dimensionless parameters for building structures

$\bar{s}$ ,  $\bar{h}$  and  $\bar{m}$  are related to each other in building structures and arbitrary combinations of these parameters are not acceptable for this kind of structures. Therefore, the mathematical relations between dimensionless parameters and building structure properties should be determined at the first stage.

Consider an  $n$ -story building structure with a square foundation and assume that the story height is equal to  $h_1$  and the foundation dimension is  $2a$ . Thus the modal height of the mass center of structure may be calculated from the following equation:

$$h = b \cdot (n \cdot h_1), \quad 0.1 \leq b \leq 0.8 \quad (1)$$

where  $b$  is the height coefficient of the effective modal mass and may take the values between 0.1 and 0.8 according to the mode number for typical building structures.

If the half-side of the foundation has a relation with story height as Eq. 2:

$$a = d \cdot h_1 \quad (2)$$

then the slenderness ratio can be defined as follows:

$$\bar{h} = \frac{h}{a} = \frac{b \cdot n \cdot h_1}{d \cdot h_1} = \frac{n \cdot b}{d} \quad (3)$$

For the models considered in this paper it is assumed that the range of  $d$  is from 1.5 to 8.

Now suppose that the modal period of the fixed base structure ( $T_f$ ) is proportional to the number of stories as follows:

$$T_f = c \cdot n, \quad 0.02 \leq c \leq 0.20 \quad (4)$$

Since  $\omega_S h$  quantifies the stiffness of the structure and  $V_S$  is related to the stiffness of the soil, the structure to soil stiffness ratio can be expressed as Eq. 5:

$$\bar{s} = \frac{\omega_f h}{V_s} = \frac{2\pi h}{T_f \cdot V_s} \tag{5}$$

Stiffness ratio can be written as Eq. 6 after substituting Eqs. 1 and 4 in Eq. 5 and simplifying:

$$\bar{s} = \frac{2\pi(b \cdot n \cdot h_1)}{c \cdot n \cdot V_s} = \frac{2\pi b \cdot h_1}{c \cdot V_s} \tag{6}$$

The mass ratio is defined as the ratio of structure’s modal mass to the mass of soil in a specific volume below the foundation that extends to a depth equal to the structure modal height (equal to the soil mass filling the volume of structure). The following equations are used to calculate the mass ratio  $\bar{m}$ :

$$m_1 = 4\rho a^2 \tag{7}$$

$$m = e \cdot n \cdot m_1 \tag{8}$$

$$\bar{m} = \frac{m}{\rho_s \cdot a^2 \cdot h} \tag{9}$$

After substituting Eqs. 1, 2, 7 and 8 in Eq. 9 and simplifying:

$$\bar{m} = \frac{enm_1}{\rho_s d^2 h_1^2 (bnh_1)} = \frac{e(4\rho d^2 h_1^2)}{\rho_s d^2 h_1^3 b} = \frac{4e\rho}{\rho_s bh_1} \tag{10}$$

where  $\rho$  is the effective mass per unit area of the story,  $\rho_s$  is the mass density of the soil and  $e$  is the coefficient of effective modal mass that may take a range of values from 0.1 to 1 according to the mode number.

### 2.2 Parametric study

There is a specific range of dimensionless parameters for a building in its different configurations and natural modes on various soils. Since these parameters are defined based on equivalent SDF system properties, the structure has to be idealized as an SDF stick model. The properties of this model such as mass, height and period are obtained from modal properties of the corresponding building and therefore each stick model is representing a mode of the same structure. Such a modeling makes it possible also to investigate the contribution level of different vibrational modes to SSI effects. Several structure and soil models are chosen on this basis. Table 2 represents these models and their corresponding dimensionless parameters. In this table, soft, medium and stiff soil conditions correspond to  $V_s \leq 175$  m/s,  $175$  m/s  $\leq V_s \leq 375$  m/s and  $375$  m/s  $\leq V_s \leq 750$  m/s respectively; low-, medium- and high-rise buildings correspond to  $1 \leq n \leq 4$ ,  $5 \leq n \leq 15$  and  $16 \leq n$ , respectively and values of the effective mass per unit area of each story varies from 500 kg/m<sup>2</sup> for light weight to 1000 kg/m<sup>2</sup> for heavy structures. Soil and structure conditions must be compatible in deriving the values of the parameters. Therefore, for example, it is considered that a shallow foundation is not appropriate for supporting mid-rise and tall buildings on soft soils. The last mode in this table represents the last important mode that has a significant effect on the dynamic response of structure.

**Table 2** Selected models and the corresponding dimensionless parameters

Model no.	Structure height	Mode	Structure weight	Horizontal dimension	Soil condition	<i>n</i>	<i>b</i>	<i>c</i>	<i>e</i>	$\rho$ (kg/m <sup>3</sup> )	<i>d</i>	<i>V<sub>s</sub></i> (m/s)	$\rho_s$ (kg/m <sup>3</sup> )	$\bar{h}$	$\bar{s}$	$\bar{m}$
1	Short	First	Light	Wide	Soft	2	0.8	0.2	0.9	500	6	100	1700	0.267	0.880	0.378
2					Stiff					2000		500	2000	0.267	0.176	0.321
3				Slender	Soft					1700	1.5	100	1700	1.067	0.880	0.378
4					Stiff					2000		500	2000	1.067	0.176	0.321
5			Heavy	Wide	Soft				1000	1700	6	100	1700	0.267	0.880	0.756
6					Stiff					2000		500	2000	0.267	0.176	0.643
7				Slender	Soft					1700	1.5	100	1700	1.067	0.880	0.756
8					Stiff					2000		500	2000	1.067	0.176	0.643
9		Last	Light	Wide	Soft		0.1	0.04	0.1	500	6	100	1700	0.033	0.550	0.336
10					Stiff					2000		500	2000	0.033	0.110	0.286
11				Slender	Soft					1700	1.5	100	1700	0.133	0.550	0.336
12					Stiff					2000		500	2000	0.133	0.110	0.286
13			Heavy	Wide	Soft				1000	1700	6	100	1700	0.033	0.550	0.672
14					Stiff					2000		500	2000	0.033	0.110	0.571
15				Slender	Soft					1700	1.5	100	1700	0.133	0.550	0.672
16					Stiff					2000		500	2000	0.133	0.110	0.571
17	Medium	First	Light	Wide	Medium	15	0.7	0.15	0.7	500	6	200	1800	1.750	0.513	0.317
18					Stiff					2000		500	2000	1.750	0.205	0.286
19				Slender	Medium					1800	3	200	1800	3.500	0.513	0.317
20					Stiff					2000		500	2000	3.500	0.205	0.286
21			Heavy	Wide	Medium				1000	1800	6	200	1800	1.750	0.513	0.635
22					Stiff					2000		500	2000	1.750	0.205	0.571
23				Slender	Medium					1800	3	200	1800	3.500	0.513	0.635
24					Stiff					2000		500	2000	3.500	0.205	0.571
25		Last	Light	Wide	Medium		0.1	0.02	0.1	500	6	200	1800	0.250	0.550	0.317
26					Stiff					2000		500	2000	0.250	0.220	0.286

**Table 2** continued

Model no.	Structure height	Mode	Structure weight	Horizontal dimension	Soil condition	$n$	$b$	$c$	$e$	$\rho$ (kg/m <sup>3</sup> )	$d$	$V_s$ (m/s)	$\rho_s$ (kg/m <sup>3</sup> )	$\bar{h}$	$\bar{s}$	$\bar{m}$
27				Slender	Medium						3	200	1800	0.500	0.550	0.317
28					Stiff							500	2000	0.5	0.220	0.286
29			Heavy	Wide	Medium				1000		6	200	1800	0.25	0.550	0.635
30					Stiff							500	2000	0.25	0.220	0.571
31				Slender	Medium						3	200	1800	0.5	0.550	0.635
32					Stiff							500	2000	0.5	0.220	0.571
33	Tall	First	Light	Wide	Medium	30	0.7	0.15	0.7	500	8	300	1900	2.625	0.342	0.301
34					Stiff							500	2000	2.625	0.205	0.286
35				Slender	Medium						4	300	1900	5.250	0.342	0.301
36			Heavy	Wide	Medium				1000		8	300	1900	5.250	0.205	0.286
37					Stiff							500	2000	2.625	0.342	0.602
38				Slender	Medium						4	300	1900	5.250	0.205	0.571
39					Stiff							500	2000	5.250	0.342	0.602
40				Wide	Medium				500		8	300	1900	5.250	0.205	0.571
41		Last	Light	Wide	Medium		0.1	0.02	0.1	500		500	2000	0.375	0.367	0.301
42					Stiff							500	2000	0.375	0.220	0.286
43				Slender	Medium						4	300	1900	0.750	0.367	0.301
44					Stiff							500	2000	0.750	0.220	0.286
45			Heavy	Wide	Medium				1000		8	300	1900	0.375	0.367	0.602
46					Stiff							500	2000	0.375	0.220	0.571
47				Slender	Medium						4	300	1900	0.750	0.367	0.602
48					Stiff							500	2000	0.750	0.220	0.571

### 3 Procedure of this study

As mentioned in Sect. 1, ELM is based on free-field analysis and is not valid in the vicinity of the structure. Therefore, the near-field method is proposed to overcome this limitation by including the SSI effects and modifying soil properties around the foundation. The following three sets of analyses are conducted in turn, in order to develop the mathematical relations for the near-field's mechanical and geometrical properties:

a) Analyzing the rigorous models (plastic models):

In the rigorous models, the soil behavior is simulated by an elastic–plastic constitutive model that is accurate enough in general loading conditions. Each one of these models is analyzed under 10 different ground motions that are selected appropriately and are imposed to the base of the models. Dimensions of a region just below the foundation, or the near-field zone, where the soil has experienced on average larger strains at a larger rate compared with the far-field zone are determined. In other words, the rate of change in shear strains of the near-field zone is considerably greater than the far-field. It is the main criterion for determining the near-field dimensions. Figure 1 shows a schematic illustration of the mentioned region. In Fig. 1,  $2a$  is the foundation width and  $L_{nf}$  and  $H_{nf}$  represent the near-field dimensions. Average of results obtained from 10 different ground motions is considered as the response of that model. More details about the soil domain, the super-structure modeling, and the boundary conditions are presented in Sect. 4.

b) Analyzing models with the near-field approach

In this case, the soil is assumed to behave linearly and have equivalent linear characteristics. Properties of the soil in both the near- and far-field zones are first obtained by free-field analysis of the site (i.e. the traditional equivalent linear method) and kept unchanged for the soil in the far-field region in the rest of analysis. Then, characteristics (shear modulus and damping) of the near-field soil are modified through a trial and error process in order to achieve the same maximum structural drift obtained in the rigorous analyses. In other words, the near-field damping is determined based on the strain level of this region and then consecutive reductions are applied on the shear modulus of the soil in the near-field zone for the structural drift to be converged to that computed with the nonlinear soil modeling. Finally, these modified shear modulus and damping are collected as the near-field properties of the considered model.

c) Regression analysis to develop mathematical relations

After obtaining the near-field properties for all of the models, regression analyses will be performed to develop mathematical relations for the near-field properties based on the dimensionless parameters of the SSI system, as introduced in Sect. 2.1.

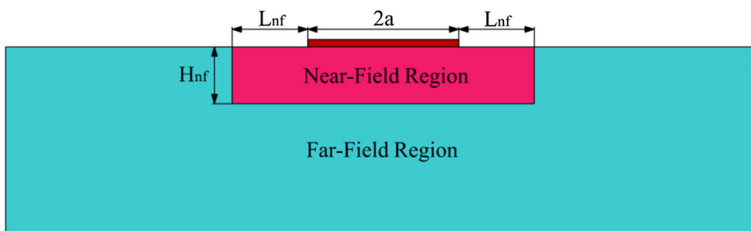


**Fig. 1** Schematic illustration of the near and far-field regions



Further explanation about modeling details and analysis steps are presented in the next sections.

## 4 Modeling details

The open source software framework OpenSees (*Open System for Earthquake Engineering Simulation*) (Mckenna 1997; Mazzoni et al. 2007) has been used to create and analyze the three dimensional FE models of this study in the time domain. The material and elements used for simulating both soil and superstructure are described in this section. In addition, the methodology used for applying gravitational and seismic loads is presented here.

### 4.1 Structure

The structure is idealized as an SDF stick model with modal properties of the building structure as shown in Fig. 2. The lumped mass,  $m$ , and the height,  $h$ , of this SDF structure are corresponding to the effective modal mass and height of the building structure. Using such a simple model clears the path to investigate the effects of the modal properties of the structure without considering any specific type of structural system. The structure model is placed at the center of a square rigid mat foundation. As a main assumption, both the structure and its foundation are supposed to have a linear elastic behavior during analysis. Elastic beam-column and shell elements are used for modeling of the structure and mat foundation, respectively.

### 4.2 Soil domain

The described SDF system is supported by a 3D soil domain and no uplift is allowed between the foundation and soil. Simulating the soil behavior is one of the major challenges in geotechnical earthquake engineering. In this study a Pressure Dependent Multi-Yield (PDMY) elastic–plastic constitutive model is used to model the soil behavior in the rigorous models. This constitutive model is capable of simulating the fundamental response characteristics (e.g. dilational behavior and cyclic mobility) of pressure sensitive soils under monotonic and cyclic loading conditions. The PDMY model has been developed by Yang et al. (2003) and was implemented in OpenSees. Values of the parameters of this model as recommended by its developers for typical soil conditions are presented in Table 3. In this table, the peak shear strain is an octahedral shear strain at which the maximum shear strength is reached; the reference pressure is a reference mean effective confining pressure at which the peak shear strain is attained; the pressure dependent coefficient is a positive constant defining variation of the shear modulus as a function of the effective confining pressure; the contraction is a non-negative constant used for defining

**Fig. 2** The idealized SDF structure and its square foundation

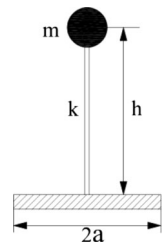


**Table 3** Values of the constitutive parameters for the soils in this study

Parameter	Value			
Site shear wave velocity (m/s)	100	200	300	500
Density (kg/m <sup>3</sup> )	1700	1800	1900	2000
Friction angle (°)	29	33	37	40
Peak shear strain	0.1	0.1	0.1	0.1
Reference pressure (kpa)	80	80	80	80
Pressure dependent coefficient	0.5	0.5	0.5	0.5
Phase transform angle (°)	29	27	27	27
Contraction	0.21	0.07	0.05	0.03
Dilation1	0	0.4	0.6	0.8
Dilation2	0	2	3	5
Initial void ratio	0.85	0.7	0.55	0.45

the rate of contraction; and finally dilation 1 and dilation 2 are non-negative constants defining the rate of shear-induced volume increase (dilation). The dilational behavior of soil is controlled by dilation 1 and dilation 2 and larger values are used for denser sands and correspond to stronger dilation rates (Mazzoni et al. 2007). This material model is used to simulate the drained soil condition.

As mentioned before, in the near-field model an equivalent linear elastic behavior is assumed for the soil and therefore a Rayleigh damping formulation should be used to include material damping in the soil domain. The full form of this formulation is expressed as Eq. 11.

$$[C] = \alpha[M] + \beta[K] \quad (11)$$

where  $[M]$  is the mass matrix,  $[K]$  is the stiffness matrix and  $\alpha$  and  $\beta$  are Rayleigh damping coefficients calculated to obtain desired damping ratios for two control frequencies (Phillips and Hashash 2009). Kwok et al. (2007) examined different frequencies and showed that using the first mode natural frequency of site and five times that frequency (presumably being equal to the third mode's natural frequency of site) gives the best match to the exact solution. Because of its wide acceptability and accuracy, recommendation of Kwok et al. (2007) is followed for the purposes of this study.

The soil domain is discretized by 8 node solid elements. The maximum element length,  $\Delta h$ , is calculated by Eq. 12 in order to avoid numerical damping (Jeremic et al. 2009).

$$\Delta h \leq \frac{\lambda_{\min}}{10} = \frac{V_s}{10f_{\max}} \quad (12)$$

where  $V_s$  is the shear wave velocity of the soil and  $f_{\max}$  and  $\lambda_{\min}$  are the highest frequency and the least wave length of the propagating waves, respectively. Typically,  $f_{\max}$  can be assumed to be equal to 10 Hz for seismic analysis. An example of the 3D FE mesh of the soil–foundation–structure (SFS) system of this study is illustrated in Fig. 3.

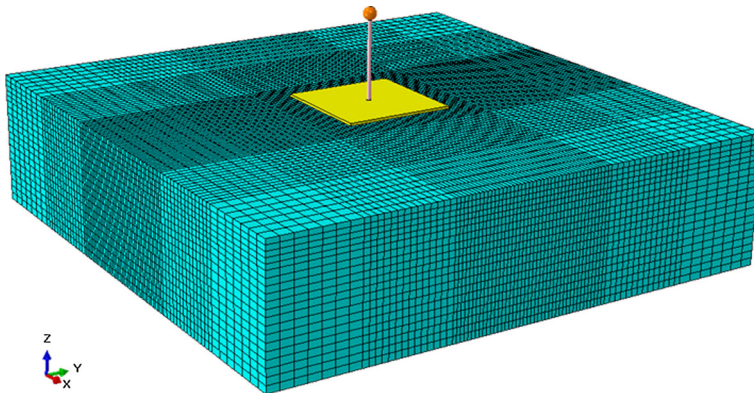


**Fig. 3** 3D FE model of the SFS system

**Table 4** The criteria for ground motion selection

Property	Value
Magnitude (Ms)	$5.5 \leq M \leq 7.5$
Source distance (km)	$\Delta \geq 15$ km
Accelerogram location	Ground surface
Average shear wave velocity of top 30 meters of the soil deposit ( $V_{s30}$ )	Consistent with each site

### 4.3 Soil medium dimensions and boundary conditions

The soil domain is semi-infinite in dimension and just a bounded cut of it can be modeled in the FE analysis. The boundaries of such a model should be able to absorb impinging waves. The boundary condition developed by Lysmer and Kuhlmeyer (1969) is used as the absorbing boundary to simulate the radiation damping.

The sensitivity analysis of the structural response to the horizontal dimension (L) of the FE model shows that for the most critical cases, the horizontal dimension of the soil domain should be at least 4 times the foundation width. In practice the soil dimension is taken to be 5 times the foundation dimension. The depth of the soil layer on a rigid base is assumed to be 50 m. This is deep enough for the boundary condition at the bottom not to affect the structural response and the strain distribution under the foundation.

## 5 Ground motions

As shown in Table 2, four different soil types are considered for this research. A set of 10 ground motions are selected from the PEER Strong Motion Database (2010) and the European Strong Motion Database (2012) for each site based on the criteria mentioned in Table 4. Characteristics of the selected ground motions are summarized in Table 5.

The selected earthquake records should be scaled to be strong enough to excite the structure more or less similarly. The ASCE7-10 (ASCE 2010) criteria and design

**Table 5** Selected ground motions for each site

Number	Event	Station	Magnitude	PGA(g)
<i>(a) <math>V_s = 100\text{ m/s}</math></i>				
1	Bucharest	Building Research Institute	7.5	0.201
2	Coalinga	Parkfield-Cholame 2WA	6.36	0.109
3	Imperial Valley	EC Meloland Overpass FF	6.53	0.314
4	Loma Prieta	APEEL2-Redwood City	6.93	0.274
5	Loma Prieta	Larkspur Ferry Terminal	6.93	0.137
6	Montenegro	Veliki Ston	6.9	0.267
7	Superstition Hills	Imperial Valley Wildlife	6.7	0.201
8	Superstition Hills	Salton Sea Wildlife Refuge	6.7	0.167
9	Westmorland	Westmorland Fire Station	5.9	0.368
10	Whittier Narrows	Carson-Water	5.99	0.133
<i>(b) <math>V_s = 200\text{ m/s}</math></i>				
1	Dinar, Turkey	Dinar	6.4	0.352
2	Imperial Valley	El Centro Array#2	6.53	0.365
3	Loma Prieta	Oakland-Outer harbor wharf	6.93	0.287
4	Loma Prieta	Palo Alto-1900 Embarc	6.93	0.213
5	Northridge	Downey Brichdale	6.69	0.165
6	Northridge	LA Century City CC North	6.69	0.250
7	Northridge	Terminal Island	6.69	0.133
8	Parkfield	Vineyard Cyn 1E	6.19	0.259
9	Superstition Hills	Calipatria Fire Station	6.7	0.247
10	Whittier Narrows	Lakewood	5.99	0.277
<i>(c) <math>V_s = 300\text{ m/s}</math></i>				
1	Hector Mine	Big Bear Lake Fire Station	7.13	0.173
2	Imperial Valley	Sahop Casa Flores	6.53	0.506
3	Kobe	Kakogawa	6.9	0.345
4	Landers	Fort Irwin	7.28	0.122
5	N Palm Springs	Hurkey creek park	6.06	0.187
6	Northridge	Buena Park-La Palma	6.69	0.139
7	Northridge	Santa Monica	6.69	0.363
8	Superstition Hills	Parachute Test Site	6.7	0.377
9	Superstition Hills	Plaster City	6.7	0.186
10	Whittier Narrows	Compton-Castlegate St.	5.99	0.332
<i>(d) <math>V_s = 500\text{ m/s}</math></i>				
1	Cape Mendocino	Shelter Cove Airport	7.01	0.189
2	Coalinga	Slack Canyon	6.36	0.166
3	Duzce	LDEO Station	7.2	0.515
4	Loma Prieta	SF-Presidio	6.93	0.2
5	Northridge	Beverly Hills-12520 Mulh	6.69	0.617
6	Northridge	Rancho Palos Verdes	6.69	0.167
7	Northridge	Sim Valley-Katherine	6.69	0.878

**Table 5** continued

Number	Event	Station	Magnitude	PGA(g)
8	Parkfield	Temblor	6.19	0.272
9	San Fernando	Santa Anita Dam	6.61	0.212
10	San Salvador	Geotech Investig Center	5.8	0.475

spectrums with  $S_5 = 1.5$  g and  $S_1 = 0.6$  g are used for this purpose. In the software, the ground motion is applied to the base of the model, but these records have been recorded on the ground surface. Therefore, a deconvolution analysis is performed beforehand to calculate the ground motion at the base level using the Shake91 software (Idriss and Sun 1992). As mentioned in Sect. 4.2, the PDMY model employs a power function to represent variation of the shear modulus as a function of the effective confining pressure. Same pattern is used to model different layers of the considered soil profile.

## 6 Solution procedure

Initial conditions are very important in simulating geotechnical phenomena; consequently a staged approach is employed in the rigorous analysis phase. The solution procedure is composed of the following three stages:

- a) The gravity load is applied to the linear soil model.
- b) The behavior of the soil elements is switched from linear elastic to elastoplastic constitutive behavior and the gravity analysis is continued until reaching equilibrium in this new state.
- c) The dynamic excitation is applied to the base of the model as an acceleration time history obtained from deconvolution analysis of the scaled ground motion.

An incremental-iterative procedure should be employed to integrate the equations of motion in the dynamic analysis phase. The Newmark method with the time integration parameters  $\gamma = 0.5$  and  $\beta = 0.25$  is used for conducting the transient analysis phase. As the previously described FE model has a large number of degrees of freedom (DOFs), the modified Newton–Raphson algorithm is utilized for decreasing the calculation cost.

The time step of the transient analysis phase ( $\Delta t$ ) has to be limited in order to assure accuracy. The time step is selected not to be larger than the time step increment of the accelerogram. In addition, an accuracy criterion is set for considering higher mode effects as follows:

$$\Delta t < \frac{T_n}{10} \quad (13)$$

here,  $T_n$  is the smallest natural period of the discretized SSI system (Jeremic et al. 2009). Another accuracy criterion arises from the nature of the FE analysis. When a wave propagates in the FE domain, it must reach one node after the previous one. With a too large time step, the wave may reach two successive nodes simultaneously. Providing for

this condition ensures that the wave can propagate in the FE domain appropriately. This criterion can be expressed by Eq. 14:

$$\Delta t < \frac{\Delta h}{V_s} \quad (14)$$

where  $\Delta h$  is the minimum element size and  $V_s$  is the shear wave velocity in the soil domain (Jeremic et al. 2009).

## 7 Time history analyses results

As mentioned in Sect. 3, 48 different SFS models are constructed for performing the parametric study and each model is subjected to 10 ground motions. Two sets of time history analyses including the rigorous (elastoplastic) and modified equivalent linear (near-field) are conducted to calculate the near-field region properties. These properties consist of the near-field dimensions, which are obtained from the rigorous analysis, and the shear modulus and damping ratio from the modified equivalent linear models analyzed with the near-field approach. Results of these analyses and their coefficients of variation (CV) are collected in Table 6. These results are the arithmetic means of the values obtained from applying 10 different ground motions to each model. Dispersion of these values is in an acceptable range because all of the ground motions are scaled to the same spectrum making them to have similar response spectrum amplitude levels. As mentioned in Sect. 3, shear strain variation around the foundation is the main criterion for determining the near-field dimensions. Therefore, shear strain distribution around the foundation is checked for each one of analyses and a region with high shear strain variation is specified as the near-field zone. For instance, the shear strain distribution and the near-field zone determination are shown for a cut of the soil domain in model No. 17 under Parkfield earthquake in Fig. 4a. The values shown in Fig. 4a are net numbers and the maximum shear strain is equal to 2.31 %. Figure 4b demonstrates variation of the normalized maximum seismic shear strain over the soil domain's depth. As can be observed in this figure, the rate of shear strain variation near the foundation is considerably greater than other regions and the near-field zone can be distinguished from the far-field. Similar analyses are performed for each model under each earthquake and the average values of the near-field dimensions are calculated. In Table 6,  $H_{N,F}/2a$  and  $L_{N,F}/2a$  are ratios of the near-field's depth and length to the foundation width, respectively,  $G/G_{Free-Field}$  represents the shear modulus reduction factor which is defined as the ratio of the near-field shear modulus (obtained from the modified equivalent linear analysis) to the shear modulus of the same region calculated by the free-field analysis of Shake, i.e. the ELM analysis, and  $\xi$  is the damping ratio of near-field region. As seen in Table 6, variation of the dimensionless parameters considerably alters the seismic response of the SSI system. A regression analysis should be performed in order to derive mathematical relations between dimensionless parameters and the near-field properties as described in the next section.

## 8 Nonlinear regression analysis

Nonlinear regression analysis should be performed for deriving the near-field properties based on the SSI characteristics including  $\bar{s}$ ,  $\bar{h}$ , and  $\bar{m}$ . Studying the impact of each one of the dimensionless parameters shows that the near-field properties are significantly sensitive to  $\bar{s}$

**Table 6** Time history analyses results: average of the results obtained from 10 different ground motions and coefficients of variation

Model no.	Plastic analysis results				Near-field analysis results			
	$(H_{NF}/2a)$	CV (%)	$(L_{NF}/2a)$	CV (%)	$(G/G_{Free-Field})$	CV (%)	$\xi$ (%)	CV (%)
1	0.200	10.00	0.508	9.62	0.333	9.21	21.0	3.97
2	0.210	7.11	0.288	6.07	0.903	7.66	4.3	5.70
3	0.350	7.14	0.510	7.36	0.484	5.16	15.5	6.61
4	0.240	6.56	0.280	5.36	0.940	7.45	3.7	8.96
5	0.230	10.25	0.468	9.78	0.305	9.64	22.0	3.52
6	0.200	7.10	0.290	7.41	0.889	4.97	4.3	9.30
7	0.330	11.44	0.480	11.62	0.476	9.54	16.5	7.78
8	0.250	8.76	0.350	9.59	0.935	5.56	3.7	10.81
9	0.210	11.81	0.486	11.25	0.362	11.38	19.5	5.73
10	0.200	8.25	0.280	8.16	0.914	6.91	4.1	7.32
11	0.300	9.07	0.500	9.10	0.515	7.48	12.0	10.54
12	0.280	8.33	0.300	7.55	0.945	8.35	3.6	12.11
13	0.226	11.44	0.530	10.90	0.362	10.97	19.5	5.73
14	0.210	8.12	0.310	8.04	0.910	6.76	4.1	7.32
15	0.280	9.77	0.520	9.52	0.505	8.73	13.0	9.10
16	0.300	7.57	0.250	7.29	0.953	6.60	3.6	10.39
17	0.215	7.65	0.252	8.25	0.626	7.53	10.2	8.55
18	0.180	7.14	0.330	6.84	0.860	8.67	4.5	9.94
19	0.300	8.62	0.375	9.99	0.676	7.25	8.8	8.50
20	0.229	8.23	0.320	8.31	0.890	9.33	4.1	11.95
21	0.167	9.12	0.262	10.65	0.610	7.58	10.1	9.34
22	0.166	7.08	0.305	7.28	0.869	7.59	4.4	8.50
23	0.310	9.83	0.395	11.35	0.642	8.50	9.0	11.39
24	0.230	7.88	0.330	9.29	0.864	6.22	4.4	11.13
25	0.188	9.47	0.350	10.83	0.540	8.36	13.3	8.27
26	0.152	7.08	0.271	8.19	0.906	5.76	4.1	7.32
27	0.320	9.79	0.433	11.11	0.577	8.87	11.9	7.93
28	0.220	6.05	0.350	6.86	0.947	5.04	3.7	12.39
29	0.190	9.55	0.350	10.49	0.536	9.30	13.1	7.97
30	0.185	7.96	0.275	8.37	0.913	8.33	4.1	7.32
31	0.320	10.01	0.424	11.28	0.563	9.23	12.0	9.86
32	0.230	8.20	0.320	9.94	0.951	5.98	3.7	10.81
33	0.150	9.08	0.250	12.09	0.763	7.86	5.4	14.22
34	0.211	7.00	0.310	8.35	0.851	7.87	4.6	8.13
35	0.250	7.44	0.330	9.96	0.785	6.22	5.0	14.83
36	0.230	9.94	0.325	12.96	0.838	9.21	4.7	13.62
37	0.160	8.13	0.240	10.30	0.751	8.02	5.5	9.96
38	0.190	6.88	0.315	8.90	0.860	6.35	4.4	12.24
39	0.261	7.88	0.335	10.15	0.770	7.42	5.1	8.55
40	0.220	7.44	0.310	9.10	0.856	7.96	4.7	11.85
41	0.170	9.21	0.280	11.83	0.724	8.85	7.0	9.58

**Table 6** continued

Model no.	Plastic analysis results				Near-field analysis results			
	$(H_{NF}/2a)$	CV (%)	$(L_{NF}/2a)$	CV (%)	$(G/G_{Free-Field})$	CV (%)	$\xi$ (%)	CV (%)
42	0.146	8.27	0.323	9.43	0.916	10.27	4.3	14.89
43	0.320	7.32	0.459	9.04	0.730	7.63	8.0	7.91
44	0.180	8.41	0.286	10.14	0.913	9.36	4.3	9.30
45	0.150	8.93	0.280	10.65	0.695	10.20	7.1	13.29
46	0.152	7.16	0.350	8.62	0.911	7.92	4.7	10.85
47	0.280	6.70	0.477	7.57	0.715	8.37	8.3	12.11
48	0.190	5.81	0.320	6.20	0.907	7.92	4.3	7.71

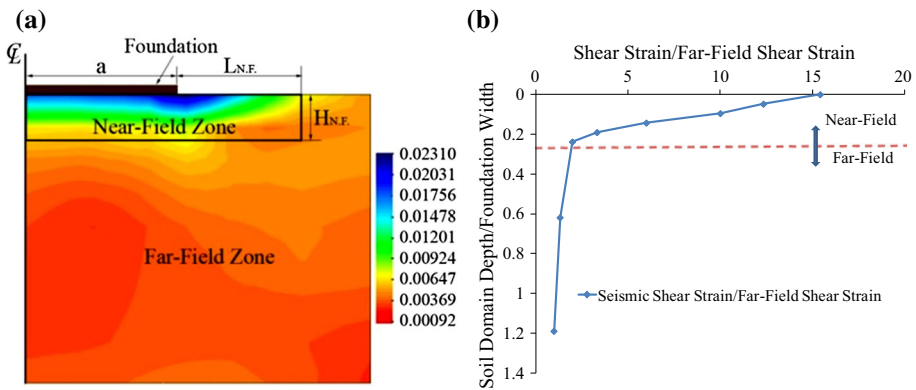


**Fig. 4** Seismic shear strain distribution and near-field zone determination for model No. 17 under Parkfield earthquake. **a** Shear strain contour. **b** Normalized maximum seismic shear strain along the soil domain depth

variation and sensitivity to  $\bar{h}$  is slightly more than  $\bar{m}$ . Moreover, based on the results presented in Table 6, it is concluded that while increase in  $\bar{s}$  and  $\bar{m}$  values increases the SSI effects, these effects decrease with increasing  $\bar{h}$ . Therefore, inertial SSI effects are directly related to  $\bar{s}$  and  $\bar{m}$  (i.e. SSI effects vary with  $\bar{s}^\alpha \times \bar{m}^\beta$ ) but they have an inverse relation with  $\bar{h}$  (i.e. SSI effects change with  $1/\bar{h}^\gamma$ ). These conclusions are consistent with the results reported by Veletsos and Meek (1974), Wolf (1985), Avilés and Pérez-Rocha (1996) and Stewart et al. (1999a, b). Accordingly, a combination in the form of  $(\bar{s}^\alpha \times \bar{m}^\beta / \bar{h}^\gamma)$  can be considered as the key parameter playing a critical role in variation of the near-field properties. Therefore this ratio is treated as an independent variable in deriving the semi-analytical relations.

Nonlinear regression analysis is conducted to determine coefficients and powers of variables in the semi-analytical relations. After performing this analysis in a sample statistical software to obtain a preliminary estimation of the coefficients and powers, a manual adjustment is also necessary to arrive at smoothed values. As of powers  $\alpha, \beta$  and  $\gamma$ , several combinations are examined and eventually the values summarized in Table 7 are proposed. These powers clearly show the level of contribution of each parameter to the SSI effects.

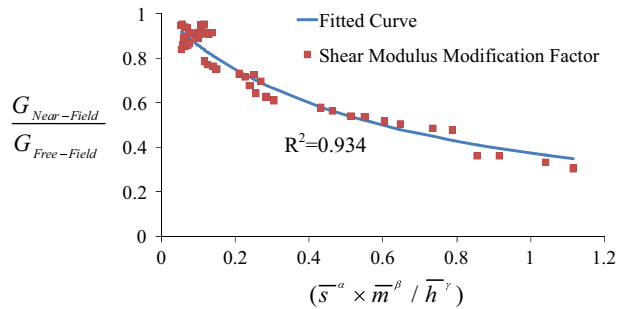
Therefore, the independent variable used for deriving all of the semi-analytical relations is  $(\bar{s}^{1.5} \times \bar{m}^{0.10} / \bar{h}^{0.25})$ . After adjusting the powers of the parameters, variation of each one



**Table 7** Powers of dimensionless parameters in the semi-analytical relations

Dimensionless parameter	Power	Value
$\bar{s}$	$\alpha$	1.5
$\bar{m}$	$\beta$	0.10
$\bar{h}$	$\gamma$	0.25

**Fig. 5** Curve fitting for the shear modulus reduction factor



of the near-field properties with respect to the considered independent variable is studied and a curve fitting technique is applied to derive the semi-analytical relations for estimating the near-field properties. More details about the proposed equations are presented in the next sections.

### 8.1 The shear modulus reduction factor

Applying the curve fitting technique to the shear modulus reduction factors leads to a function as Eq. 15.

$$\frac{G_{Near-Field}}{G_{Free-Field}} = \frac{0.6}{\left(\frac{\bar{s}^{1.5} \times \bar{m}^{0.10}}{\bar{h}^{0.25}}\right) + 0.6}, \quad R^2 = 0.934 \tag{15}$$

where  $G_{Near-Field}$  is the final shear modulus of the near-field zone,  $G_{Free-Field}$  is the effective shear modulus for the top layer of soil obtained from ELM analysis of the free-field with Shake91 and  $R^2$  is the coefficient of determination that indicates how well data fit the proposed semi-analytical model. The mathematical form of Eq. 15 is selected in such a way that it tends to unity and zero for decreasing and increasing  $(\bar{s}^\alpha \times \bar{m}^\beta / \bar{h}^\gamma)$  respectively. Figure 5 illustrates the curve fitting for the shear modulus reduction factor of the near-field zone.

### 8.2 The damping ratio

The semi-analytical relation resulted from curve fitting for estimating damping ratio of near-field zone is as Eq. 16.

**Fig. 6** Curve fitting for the damping ratio of the near-field zone

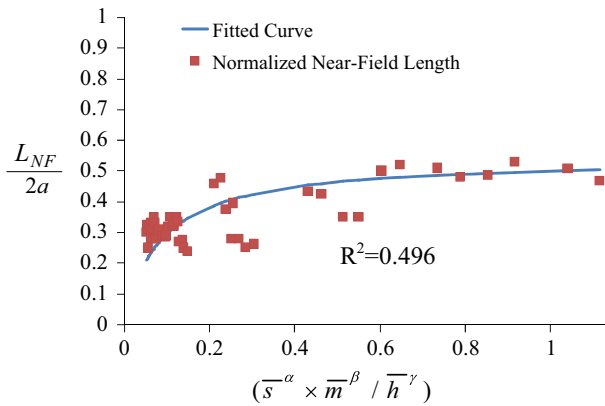
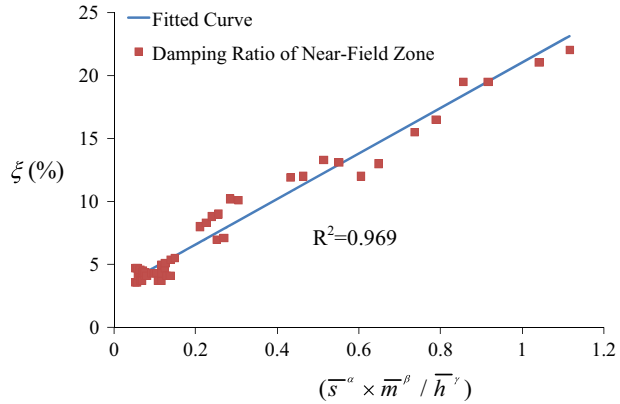


**Fig. 7** Curve fitting for the normalized near-field partial length

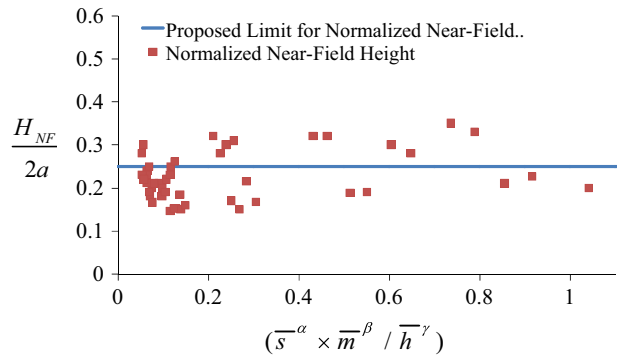
$$\xi = 18 \left( \frac{\bar{s}^{1.5} \times \bar{m}^{0.10}}{\bar{h}^{0.25}} \right) + 3, \quad R^2 = 0.969 \tag{16}$$

where  $\xi$  is the damping ratio of the near-field zone in percent. Figure 6 demonstrates the curve fitting for the damping ratio of the near-field zone.

**8.3 The near-field dimensions**

Part of the horizontal dimension (length) of the near-field protruding from each side of the foundation (see Fig. 1),  $L_{NF}$ , normalized to the foundation dimension is estimated by Eq. 17 with its curve fitting being presented in Fig. 7.

**Fig. 8** Curve fitting for the depth of the near-field zone



$$\frac{L_{N.F.}}{2a} = \frac{3.25 \left( \frac{\bar{s}^{1.5} \times \bar{m}^{0.10}}{\bar{h}^{0.25}} \right)}{6 \left( \frac{\bar{s}^{1.5} \times \bar{m}^{0.10}}{\bar{h}^{0.25}} \right) + 0.5}, \quad R^2 = 0.496 \tag{17}$$

Finally, a criterion for the depth of the near-field zone is set as:

$$H_{N.F.} = 0.25(2a) = 0.5a \tag{18}$$

where  $2a$  is the foundation width. Figure 8 illustrates the proposed equation for the near-field depths of all of the analyzed models. It should be noted that the slight discrepancies in the near-field dimensions will be shown to have no significant effects on the structural responses.

### 9 Steps of employing the near-field method

In the previous sections details of the near-field method proposed in this study were explained. As mentioned before, this method is based on decomposition of the soil domain into near-field and far-field regions and proposes modified properties for modeling of the soil in the near-field zone. This section presents a step-by-step methodology for employing the near-field method in direct SSI analysis. The main steps of the near-field method can be summarized as follows: (1) modal analysis of the fixed-base structure; (2) determining the important modes based on modal participation factors; (3) calculating  $\bar{s}$ ,  $\bar{h}$  and  $\bar{m}$  values for important modes (Eqs. 3, 5, and 9); (4) using Eqs. 15 and 16 to calculate the shear modulus modification factor and damping ratio of the near-field region for important modes, (5) computing weighted average of the shear modulus modification factor and damping ratio using the modal mass participation factor as the weight; (6) using Eqs. 17 and 18 to determine the near-field region dimensions; (7) performing free-field analysis to calculate effective soil properties under the considered earthquake and assigning effective properties to the far-field zone; (8) modifying the effective properties of the near-field zone using the modification factors obtained in step 5 and the characteristics calculated in step 7.

More details about the numerical implementation and examples are given in a companion paper.

**Table 8** Shear modulus modification factors suggested by ASCE 7-10 (ASCE 2010), FEMA P-750 (2009) and NIST (2012)

Site	Shear modulus modification factor		
	$S_{DS}/2.5$		
	$\leq 0.1$	0.4	$\geq 0.8$
A	1.00	1.00	1.00
B	1.00	0.95	0.90
C	0.95	0.75	0.6
D	0.90	0.50	0.10
E	0.60	0.05	Site-specific analysis
F	Site-specific analysis	Site-specific analysis	Site-specific analysis

**Table 9** Comparison between modulus degradation values proposed by the near-field method and the codes

Shear wave velocity of the considered sites	Near-field method	Codes
500	0.56	0.75
300	0.29	0.50
200	0.16	0.50
100	0.04	0.05

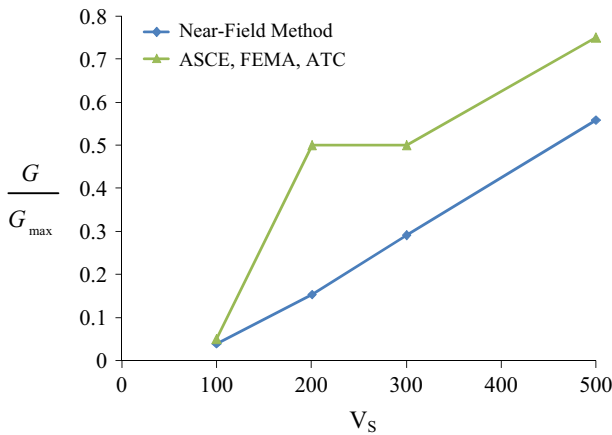


**Fig. 9** Comparison between the modulus reduction factors suggested by the near-field method and the codes

### 10 Comparison with other suggestions

There are other suggestions available in different references for modulus degradation and damping factors of the free-field soil under intensive shakings. In this section, results of the present study are compared with other available data.

**Fig. 10** Comparison between the near-field and Seed and Idriss modulus reduction values

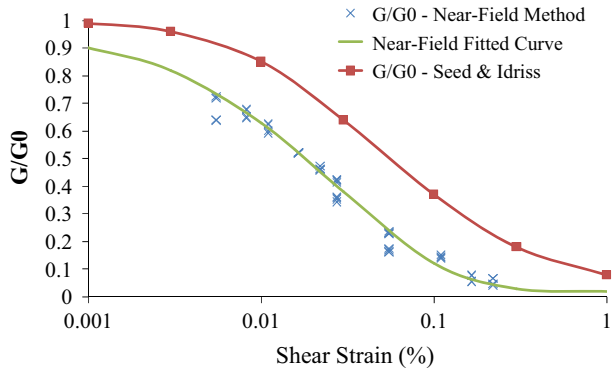
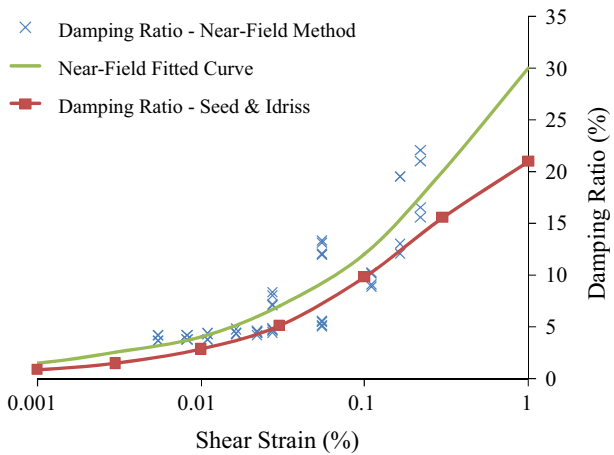


**Fig. 11** Comparison between the near-field and Seed and Idriss damping ratios



**10.1 Comparison with the building codes and references**

Some of the building codes and references such as ASCE 7-10 (ASCE 2010), FEMA P-750 (2009) and NIST (2012) present the shear modulus modification factors in a tabular form for various site and excitation conditions to take the effect of large strains induced by the design earthquake motion into account, such as Table 8. These factors are used to modify average shear modulus of soil for calculating the foundation stiffnesses. The value of  $S_{Ds}/2.5$  for considered site conditions of this research is equal to 0.4 and thus the middle column of the table is applicable for the sites of this study. On the other hand, different modulus reduction factors have been obtained by employing the near-field method for each one of the assumed site conditions and the average value of these values in each site is assumed to be a representative value for that site. Comparison between the code values and those of the near-field method is demonstrated in Table 9 and Fig. 9.

It is seen that the values of the near-field modification factors calculated in this study are smaller than those suggested by the codes. It is expected, because the code values are for the free-field conditions and no account has been given in their development for presence of a structure.

## 10.2 Comparison with Seed and Idriss modulus degradation and damping curves

Seed and Idriss (1970) used experimental data and proposed modulus degradation and damping ratio curves for sandy and clayey soils. The near-field modulus reduction and damping ratio values are compared with those suggested by Seed and Idriss in Figs. 10 and 11. It should be noted that Seed and Idriss curves are used in ELM analysis of the free-field with Shake91 and the horizontal axis represents the effective shear strain of soil in the near-field region obtained from these ELM analyses. Again, it is seen that to account for the large strains induced in the near-field, the shear modulus and damping ratios have to take smaller/larger values than those suggested by Seed and Idriss, respectively.

## 11 Conclusions

The main objective of this research was developing a simple model for the direct analysis of the soil–structure interaction including the effects of structure on the adjacent bearing soil. It was shown that a limited region in the vicinity of the foundation experiences large strains and a high level of nonlinearity to the extent that the equivalent linear method (ELM) was not accurate enough for this region. This region was called the near-field zone and it was suggested to modify its mechanical properties to resolve the limitation of ELM and take the effects of the large strains into account. The dimensionless parameters controlling the response of the dynamic soil–structure system were utilized to derive equations for the characteristics of the near-field zone. A comprehensive parametric study was conducted in a rigorous model using an elastoplastic (PDMY) constitutive relation for the underlying soil. 10 consistent ground motions were selected and applied to the model. In addition, in an equivalent linear parallel model, the characteristics of the near-field soil were tuned by trial and error to arrive at maximum structural responses equal to those of the rigorous model. After that, nonlinear regression analysis was performed and semi-analytical equations were derived for calculating the near-field properties as well as its dimensions. Comparing the reduction factors obtained in the present study with the recommendations of building codes such as ASCE 7-10 (ASCE 2010) and modulus degradation curves proposed by Seed and Idriss showed that the mechanical properties of the near-field zone have to be adopted as smaller than those of the nearby free-field zone because of the inertial effects of the structure. Inclusion of such an effect is the unique feature of the current study.

In this paper only the procedure and equations for further modification of the soil properties in the near field were given. In a companion paper (part II of the current paper), the structural responses are presented and effects of different approaches including the near-field method are discussed and compared with the available recorded data in real buildings.

## References

- Allotey N, El Naggar MH (2008) Generalized dynamic Winkler model for nonlinear soil–structure interaction analysis. *Can Geotech J* 45:560–573
- Andersen L, Jones CJC (2006) Coupled boundary and finite element analysis of vibration from railway tunnels—a comparison of two- and three-dimensional models. *J Sound Vib* 293(3):611–625

- ASCE/SEI 7-10 (2010) Minimum design loads for buildings and other structures. American Society of Civil Engineers (ASCE), Virginia
- Avilés J, Pérez-Rocha LE (1996) Evaluation of interaction effects on the system period and the system damping due to foundation embedment and layer depth. *Soil Dyn Earthq Eng* 15(1):11–27
- Baziyar MH, Song C (2006) Time-harmonic response of non-homogeneous elastic unbounded domains using the scaled boundary finite-element method. *Earthq Eng Struct Dyn* 35(3):357–383
- Bielak J (1975) Dynamic behavior of structures with embedded foundations. *Earthq Eng Struct Dyn* 3(3):259–274
- Boulanger RW, Currans CJ, Kutter BL, Wilson DW, Abghari A (1999) Seismic soil–pile–structure interaction experiments and analyses. *J Geotech Geoenviron Eng* 125:750–759
- Bozorgnia Y, Bertero VV (2004) Earthquake engineering from engineering seismology to performance-based engineering. CRC Press, New York
- Casciati S, Borja RI (2004) Dynamic FE analysis of South Memnon Colossus including 3D soil–foundation–structure interaction. *Comput Struct* 82(20):1719–1736
- Chatzigogos CT, Pecker A, Salençon J (2009) Macroelement modeling of shallow foundations. *Soil Dyn Earthq Eng* 29(5):765–781
- Chatzigogos CT, Figini R, Pecker A, Salençon J (2011) A macroelement formulation for shallow foundations on cohesive and frictional soils. *Int J Numer Anal Methods Geomech* 5(8):902–931
- Chen X, Birk C, Song C (2015) Transient analysis of wave propagation in layered soil by using the scaled boundary finite element method. *Comput Geotech* 63:1–12
- Cremer C, Pecker A, Davenne L (2001) Cyclic macro-element for soil–structure interaction: material and geometrical non-linearities. *Int J Numer Anal Methods Geomech* 25(13):1257–1284
- Cubrinovski M, Ishihara K (2004) Simplified method for analysis of piles undergoing lateral spreading in liquefied soils. *Soils Found* 44(5):119–133
- Elgamal A, Yan L, Yang Z, Conte JP (2008) Three-dimensional seismic response of Humboldt Bay bridge-foundation-ground system. *J Struct Eng* 134(7):1165–1176
- FEMA P-750 (2009) NEHRP recommended seismic provisions for new buildings and other structures. Federal Emergency Management Agency, Washington
- Figini R, Paolucci R, Chatzigogos CT (2012) A macro-element model for non-linear soil–shallow foundation–structure interaction under seismic loads: theoretical development and experimental validation on large scale tests. *Earthq Eng Struct Dyn* 41(3):475–493
- Gajan S, Kutter BL (2008) Capacity, settlement, and energy dissipation of shallow footings subjected to rocking. *J Geotech Geoenviron Eng* 134(8):1129–1141
- Gazetas G (ed) (1991) Foundation vibrations. In: *Foundation engineering handbook*. Springer, New York, pp 553–593
- Genes MC, Kocak S (2005) Dynamic soil–structure interaction analysis of layered unbounded media via a coupled finite element/boundary element/scaled boundary finite element model. *Int J Numer Methods Eng* 62(6):798–823
- Ghandil M, Behnamfar F (2015) The near-field method for dynamic analysis of structures on soft soils including inelastic soil–structure interaction. *Soil Dyn Earthq Eng* 75:1–17
- Gutierrez JA, Chopra AK (1978) A substructure method for earthquake analysis of structures including structure–soil interaction. *Earthq Eng Struct Dyn* 6(1):51–69
- Houlsby GT, Cassidy MJ (2002) A plasticity model for the behaviour of footings on sand under combined loading. *Géotechnique* 52(2):117–129
- Idriss IM, Sun JI (1992) SHAKE91: a computer program for conducting equivalent linear seismic response analyses of horizontally layered soil deposits. Center for Geotechnical Modeling, Department of Civil and Environmental Engineering, University of California, Davis
- Ishihara K (1996) Soil behaviour in earthquake geotechnics. Clarendon Press, Oxford
- Jeremic B, Guanzhou J, Preisig M, Tafazzoli N (2009) Time domain simulation of soil–foundation–structure interaction in non-uniform soils. *Earthq Eng Struct Dyn* 38(5):699–718
- Kramer SL (1996) Geotechnical earthquake engineering. Prentice-Hall civil engineering and engineering mechanics series. Prentice Hall, Upper Saddle River (c1996, 1)
- Kwok AO, Stewart JP, Hashash YM, Matasovic N, Pyke R, Wang Z, Yang Z (2007) Use of exact solutions of wave propagation problems to guide implementation of nonlinear seismic ground response analysis procedures. *J Geotech Geoenviron Eng* 133(11):1385–1398
- Lysmer J, Kuhlmeyer RL (1969) Finite dynamic model for infinite media. *J Eng Mech Div* 95(4):859–877
- Manna B, Baidya DK (2010) Dynamic nonlinear response of pile foundations under vertical vibration—theory versus experiment. *Soil Dyn Earthq Eng* 30(6):456–469

- Matlock H (1970) Correlations for design of laterally loaded piles in soft clay. In: Second Annual Offshore Technology Conference. American Society of Civil Engineers (ASCE), Texas, pp 77–94, 22–24 April 1970
- Mazzoni S, McKenna F, Scott MH, Fenves GL, Jeremic B (2007) OpenSees command language manual. Pacific Earthquake Engineering Research Center, University of California at Berkeley
- Mckenna FT (1997) Object-oriented finite element programming: frameworks for analysis, algorithms and parallel computing. Ph.D. Dissertation, University of California Berkeley
- Mylonakis G, Nikolaou S, Gazetas G (2006) Footings under seismic loading: analysis and design issues with emphasis on bridge foundations. *Soil Dyn Earthq Eng* 26(9):824–853
- National Institute of Standards and Technology (2012) NIST GCR 12-917-21 (ATC-83): soil–structure interaction for building structures. NEHRP Consultants Joint Venture, Gaithersburg, MD
- Nogami T, Otani J, Konagai K, Chen HL (1992) Nonlinear soil–pile interaction model for dynamic lateral motion. *J Geotech Eng* 118(1):89–106
- Pais A, Kausel E (1988) Approximate formulas for dynamic stiffnesses of rigid foundations. *Soil Dyn Earthq Eng* 7(4):213–227
- PEER Strong Motion Database (2010). <http://peer.berkeley.edu/smcat/>
- Penzien J (1970) Soil–pile–foundation interaction. In: Wiegel RL (ed) *Earthquake engineering*. Prentice Hall, New York
- Phillips C, Hashash YM (2009) Damping formulation for nonlinear 1D site response analyses. *Soil Dyn Earthq Eng* 29(7):1143–1158
- Raychowdhury P (2008) Nonlinear winker-based shallow foundation model for performance assessment of seismically loaded structures. Ph.D. Dissertation, University of California San Diego
- Romero A, Galvín P, Domínguez J (2013) 3D non-linear time domain FEM–BEM approach to soil–structure interaction problems. *Eng Anal Bound Elem* 37(3):501–512
- Seed HB, Idriss IM (1970) Soil moduli and damping factors for dynamic response analyses. In: Report No. EERC 70-10. Earthquake Engineering Research Center, University of California, Berkeley, CA
- Spyrakos CC, Xu C (2004) Dynamic analysis of flexible massive strip–foundations embedded in layered soils by hybrid BEM–FEM. *Comput Struct* 82(29):2541–2550
- Stewart JP, Fenves GL, Seed RB (1999a) Seismic soil–structure interaction in buildings. I: Analytical methods. *J Geotech Geoenviron Eng* 125(1):26–37
- Stewart JP, Seed RB, Fenves GL (1999b) Seismic soil–structure interaction in buildings. II: Empirical findings. *J Geotech Geoenviron Eng* 125(1):38–48
- The European Strong-Motion Database (2012). <http://www.isesd.hi.is/ESDLocal/frameset.htm>
- Vasilev G, Parvanova S, Dineva P, Wuttke F (2015) Soil–structure interaction using BEM–FEM coupling through ANSYS software package. *Soil Dyn Earthq Eng* 70:104–117
- Veletsos AS, Meek JW (1974) Dynamic behaviour of building–foundation systems. *Earthq Eng Struct Dyn* 3(2):121–138
- Veletsos AS, Nair VV (1975) Seismic interaction of structures on hysteretic. *J Struct Div* 101(1):109–129
- Von Estorff O, Firuziaan M (2000) Coupled BEM/FEM approach for nonlinear soil/structure interaction. *Eng Anal Bound Elem* 24(10):715–725
- Von Estorff O, Kausel E (1989) Coupling of boundary and finite elements for soil–structure interaction problems. *Earthq Eng Struct Dyn* 18(7):1065–1075
- Wolf JP (1985) *Dynamic soil–structure interaction*. Prentice Hall Int, Upper Saddle River
- Wolf JP (2003) *The scaled boundary finite element method*. Wiley, New York
- Wolf JP, Song C (1996) *Finite-element modelling of unbounded media*. Wiley, Chichester
- Yang Z, Elgamal A, Parra E (2003) Computational model for cyclic mobility and associated shear deformation. *J Geotech Geoenviron Eng* 129(12):1119–1127
- Yazdchi M, Khalili N, Valliappan S (1999) Dynamic soil–structure interaction analysis via coupled finite-element–boundary-element method. *Soil Dyn Earthq Eng* 18(7):499–517
- Yim SCS, Chopra AK (1985) Simplified earthquake analysis of multistory structures with foundation uplift. *J Struct Eng* 111(12):2708–2731